

Novel Polarization Conversion Effect in Polarization Volume Gratings for Waveguide-Based AR Displays

Yuqiang Ding, Yefu Zhang, Yongziyan Ma, Yuge Huang, Shin-Tson Wu

College of Optics and Photonics, University of Central Florida, Orlando, FL 32816, USA

E-mail: yuqiang.ding@ucf.edu, Phone: +1 407-409-3289

Abstract

To circumvent the low efficiency of waveguide-based AR displays, we discovered a novel polarization conversion effect in polarization volume gratings. Leveraging from this effect, we break the theoretical in-coupling efficiency limit of conventional couplers. In the experiment, we achieved a 2x higher optical efficiency and 2.3x better eyebox uniformity.

Author Keywords

Near-eye display; Augmented reality; waveguide displays; polarization volume gratings.

1. Introduction

Augmented reality (AR) has evolved from a futuristic concept into a pervasive technology, driven by advancements in microdisplay technologies, ultracompact optics, and high-speed processors. By blending virtual content with real-world scenes, AR enhances our perception and interaction with the environment, enabling applications in fields such as education, healthcare, navigation, gaming, and manufacturing. Since its early development in the 1990s, AR has made significant progress, especially with the advent of waveguide-based displays that offer lightweight, slim designs without sacrificing optical performance. Additionally, innovations in couplers such as partial reflective mirrors, surface relief gratings (SRGs), volume holographic gratings (VHG), polarization volume gratings (PVGs), and metasurfaces have further improved AR display performance [1-3].

While waveguide displays have dramatically reduced the formfactor, the low efficiency of optical combiners, particularly the diffractive waveguide combiners, remains a major concern. In the era of modern wireless near-eye displays powered by batteries, such a low optical efficiency imposes a significant challenge, ultimately limiting the continuous operation time.

As analyzed in our recent work [4], the low optical efficiency primarily stems from four aspects, all related to the nonuniformity issues, such as color nonuniformity, FoV nonuniformity, and eyebox nonuniformity. The first major optical loss results from the absorption and scattering of a high-index waveguide substrate. The second major source of optical loss occurs during the pupil expansion process. A significant portion of light is wasted due to the spatially limited bandwidth modulation capability of the folding couplers and out-couplers. The third major cause of light loss is the limited angular and spectral bandwidth of couplers at high diffraction efficiency. As the FoV increases, the coupler's bandwidth may not be sufficient to maintain a good uniformity. To improve uniformity, lower efficiency couplers are often compromised to achieve a broader bandwidth. Importantly, a larger FoV exacerbates energy loss during this process. As depicted in Fig. 1(a), the fourth major cause of low efficiency originates from multiple interactions at the in-couplers [5-6]. Significant light leakage occurs at the in-coupler to maintain a good eyebox uniformity, even when the in-coupler is a fully reflective mirror or

a grating with 100% diffraction efficiency.

The issue of light leakage at the in-coupler has been noticed over the past few decades, yet no couplers can completely resolve this tough problem because it is fundamentally unavoidable with conventional in-couplers, including SRG, intensity-type VHG, and even metasurface devices. Recent studies [6] have indicated that the second interaction mirrors the symmetric process of the first interaction, implying that almost all the light experiencing the second interaction will either be coupled out of the waveguide or change its propagation direction if the diffraction efficiency is 100%. As further examined in conventional couplers (Fig. 1(b)), the second interaction is essentially a reversed process of the first interaction. This is primarily because conventional couplers are made of isotropic materials, resulting in no polarization changes during the interaction process.

As depicted in Fig. 1(a), if the size (W) of the in-coupler is greater than the total internal reflection (TIR) propagation distance $d = 2t * \tan(\theta)$, where t represents the waveguide thickness and θ denotes the TIR angle inside the waveguide, then the in-coupling light will interact with the in-coupling grating two or more times. In practical terms, achieving a continuous eyebox necessitates that $W > d$. Otherwise, the user may not perceive digital information in certain regions within the eyebox. Thus, even if the width of the in-coupler can be reduced by increasing the collecting power of the collimation lenses or shrinking the emission cone of the microdisplay panels, the TIR angle θ or waveguide thickness t must be decreased accordingly to maintain a good continuity throughout the eyebox. Consequently, the efficiency loss and poor uniformity throughout the FoV persist as significant challenges.

Therefore, finding a solution to circumvent the tradeoff between in-coupling efficiency, uniformity throughout the FoV, and eyebox continuity is urgently needed.

In this paper, we present the discovery and investigation of a novel polarization conversion phenomenon in the polarization volume gratings. Our analysis reveals that such a polarization conversion is inherently tied to all cholesteric liquid crystal (CLC)-based devices, including CLC reflectors and CLC-based polarization volume holograms. We find that this phenomenon is triggered by the transition of eigenstates from circular polarization to linear polarization as the incident angle deviates from the helical axis. In waveguide displays, this phenomenon offers an intuitive solution to the abovementioned issue for achieving a high and uniform in-coupling efficiency throughout the entire FoV while maintaining continuous eyebox functionality. Leveraging such a novel polarization conversion effect in PVG, the in-coupling efficiency limit of a 50° FoV waveguide-based AR display system is enhanced by 2x with the first-order novel polarization conversion in PVG, compared to conventional couplers. Concurrently, the uniformity throughout the FoV is also improved by 2.3x.

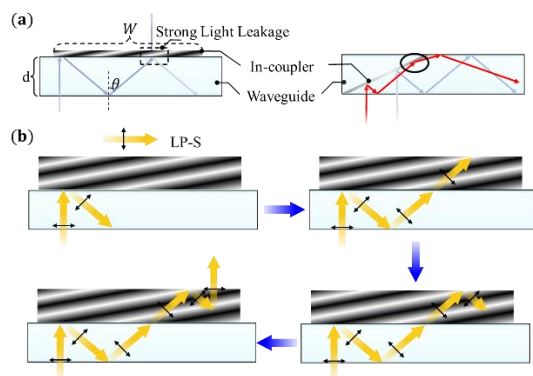


Figure 1. Light loss mechanisms in the in-coupler of waveguide-based AR displays. (a) Light loss due to multiple interactions at the diffractive in-coupler and geometric in-coupler; (b) Multiple interaction processes between the incident beam and the intensity-type VHG in-coupler.

2. Working principles

The PVG is a polarization-selective holographic optical element that records the polarization information of two interfering beams comprising a right-handed circular polarization (RCP) and a left-handed circular polarization (LCP). As illustrated in Fig. 2(a), PVG features a slanted CLC structure, where the liquid crystal (LC) directors rotate along the helical axis [7-8]. This CLC structure endows PVG with the polarization-selective characteristic of CLC, as depicted in Fig. 2(a). It reflects the circular polarization state possessing the same handedness as the helical twist of the CLC, while transmitting the opposite component. For example, it diffracts the LCP while transmitting the RCP. Additionally, the first order diffraction efficiency (R_1) increases with the CLC pitch number and then gradually saturates.

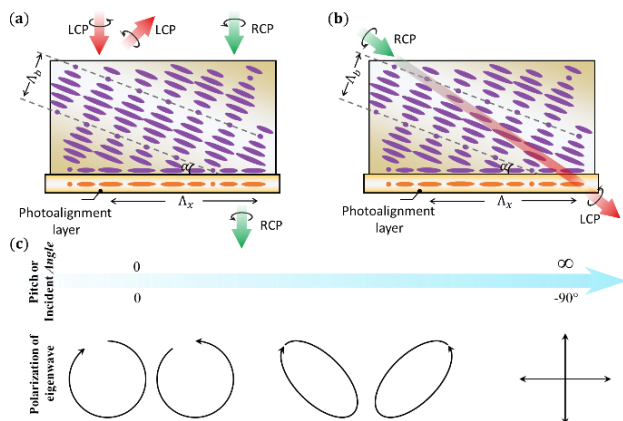


Figure 2. Working principles of polarization conversion in PVG. (a) Slanted structure of PVG, which reflects LCP and transmits RCP. (b) PVG functions as a waveplate when the incident angle of light approaches the Bragg plane. (c) Evolution of liquid crystal structures and the polarization of their corresponding eigenwaves with varying pitch or incident angles relative to helix axis.

However, we discovered a novel polarization phenomenon that deviates from the abovementioned rule [4, 9]. As depicted in Fig. 2(b), when the incident angle in the glass substrate approaches the Bragg plane and the incident light may no longer satisfy the Bragg conditions, which in turn experiences a phase mismatch described by following equation:

$$|n_{in} \sin \theta_{in} - \frac{\lambda}{\Lambda_x}| > |n_{out}|, \quad (1)$$

where n_{in} and n_{out} are the refractive indices of the input and output media, θ_{in} is the incident angle, λ is the wavelength, and Λ_x is the horizontal period of the PVG. Consequently, nearly all light will pass through the PVG. Besides, by solving the Maxwell equations for CLC reflectors, we found out that the eigenwaves will gradually transit from circular polarization states to linear polarization states as the pitch becomes longer or the incident angle deviates from the helix axis of CLC-based devices as shown in Fig. 2(c). Therefore, the PVG also functions as a waveplate altering the polarization state of the incident light at the large incident angle. For instance, it converts RCP to LCP when the half-wave condition is satisfied as shown in Fig. 2(b).

To demonstrate the polarization conversion phenomenon, the 0th order transmission efficiency and output polarization state are simulated using the RCWA model [10]. For example, when the incident angle is relatively small (e.g., $\theta = -11^\circ$ in the glass with a refractive index of 1.57), the incident light perceives a longer pitch, as illustrated in Fig. 2(b). The simulation results in Fig. 3(a) indicate that the Stokes parameter S_3 oscillates from -1 to a value less than 1 as the PVG thickness increases, suggesting that the eigenwaves exhibit an elliptical polarization state. As Fig. 3(b-d) shows, increasing the incident angle allows the Stokes parameters to transition gradually from -1 to 1, indicating a shift of eigenstates toward a linearly polarized light (s and p waves). Notably, the simulation reveals that PVG can achieve a complete circular polarization conversion at a smaller incident angle. This is primarily due to the slanted structure of the PVG, which provides a wider angular range for achieving a complete polarization conversion, thereby significantly enhancing the in-coupling efficiency in waveguide-based AR displays, which will be explained later.

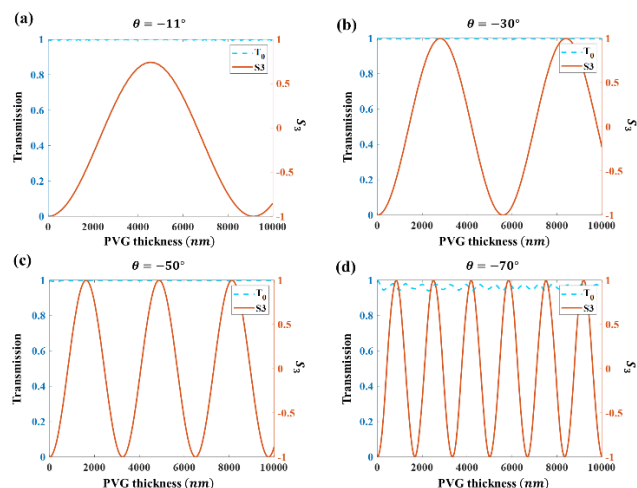


Figure 3. Polarization conversion of PVG at large incident angles. Simulated PVG thickness dependent polarization conversion at incident angle (a) $\theta = -11^\circ$, (b) $\theta = -30^\circ$, (c) $\theta = -50^\circ$, and (d) $\theta = -70^\circ$ in the glass substrate, for a wavelength of 532 nm. The horizontal period and slanted angle of the PVG is 400 nm and 28.96° , respectively, and the LC refractive indices are $n_e = 1.7$ and $n_o = 1.5$.

Furthermore, we also investigate the angular and spectral responses of PVGs. The results above indicate that PVGs can achieve a complete circular polarization conversion at multiple optimal thicknesses, akin to multiple-order half-wave phase retardations. However, as the order of phase retardation increases,

corresponding to a greater optical thickness, the angular and spectral bandwidths of the circular polarization conversion become narrower. As shown in Fig. 4(a-b), a PVG at the first optimal thickness (first-order half-wave phase retardation) exhibits a significantly broader angular and spectral bandwidth compared to a PVG at the second optimal thickness (second-order half-wave phase retardation). However, neither can convert the polarization in the entire TIR angles for the visible light. Additionally, like a conventional half-wave plate, increasing the LC birefringence does not expand the angular or spectral bandwidth. However, it does reduce the optical thickness required for each order of half-wave phase retardation, thereby lowering the fabrication complexity of PVGs. This is crucial since a thicker PVG film is more difficult to align well due to the limited anchoring energy provided by the photoalignment layer.

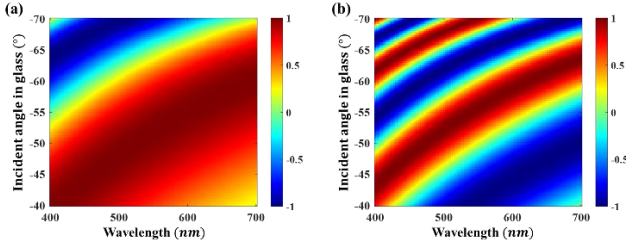


Figure 4. Angular and spectral response of polarization conversion at (a) first-order half-wave phase retardation at PVG thickness of $1.6 \mu\text{m}$ and (b) second-order phase retardation at PVG thickness of $4.3 \mu\text{m}$. The horizontal period and slanted angle of the PVG is 400 nm and 28.96° , respectively, and the LC refractive indices are $n_e = 1.7$ and $n_o = 1.5$.

Due to these two superior polarization properties, employing PVG as an in-coupler in waveguide displays can dramatically enhance the in-coupling efficiency and uniformity throughout the FoV, while keeping a good eyebox continuity (or uniformity), in comparison with all other traditional in-couplers and metasurface couplers. Specifically, as illustrated in Fig. 5(a), the incident LCP light is deflected into the waveguide substrate during the first interaction and retains its polarization state based on the selectivity rule of PVG. After the first interaction, following TIR, the polarization state of light becomes RCP (the 1st green arrow) due to the reversed propagation direction. During the second interaction with the in-coupler (PVG), the light undergoes polarization conversion without altering its propagation direction, meaning the light turns to LCP if the PVG thickness satisfies the half-wave condition. Subsequently, after another TIR at the top boundary of the PVG, the light becomes RCP, which is then transmitted through the PVG due to its polarization selectivity. Finally, the light can propagate inside the waveguide while maintaining its propagation direction. Consequently, the in-coupling efficiency and uniformity are significantly improved while maintaining a desired eyebox continuity.

3. Results and Discussion

To validate the concept, we also investigate the first-order polarization conversions in a PVG-based waveguide display with $50^\circ [30^\circ (\text{H}) \times 40^\circ (\text{V})]$ diagonal FoV at $\lambda = 532 \text{ nm}$ through polarization raytracing. It demonstrates significant enhancements in in-coupling efficiency and uniformity throughout the entire FoV, surpassing the theoretical in-coupling efficiency limit of conventional diffractive in-couplers.

Before conducting polarization raytracing, the system configuration and parameters must be designed meticulously,

including the display panel, collimation lens, in-coupler, and out-coupler. For the light engine, we assume that the in-coupler of the waveguide display (or exit pupil of the light engine) is a circle with a diameter $W = 3 \text{ mm}$, which depends on the design of the collimation lens and the emission cone of the display panel. In most waveguide-based displays, the emission cone is typically very small, around $\pm 15^\circ$. For our calculations, we employ an ideal lens as the collimation lens. Therefore, the focal length of the collimation lens (CL) can be calculated as follows:

$$f = W / (2 \tan(15^\circ)) = 5.598 \text{ mm} \quad (2)$$

Moreover, to achieve a diagonal FoV of $50^\circ [30^\circ (\text{H}) \times 40^\circ (\text{V})]$, the panel size is set to $3 \text{ mm} \times 4.075 \text{ mm}$. Subsequently, a waveguide substrate with thickness $t = 0.55 \text{ mm}$ and index $n = 1.7$ is utilized for design and simulation. Furthermore, to ensure a continuous eyebox, we assume that the pupil is continuous at the maximum TIR angle θ_{max} . This implies that each TIR propagation distance d at the maximum TIR angle is equal to the in-coupler size W , as illustrated in Fig. 4(b). Based on following equation:

$$d = 2t * \tan \theta_{\text{max}} = W \quad (3)$$

the maximum TIR angle is around 70° . Therefore, the minimum TIR angle $\theta_{\text{min}} = 38^\circ$ and the horizontal period $\Lambda_x \cong 407 \text{ nm}$ of the in-coupler and out-coupler can be derived from the FoV = $50^\circ [30^\circ (\text{H}) \times 40^\circ (\text{V})]$.

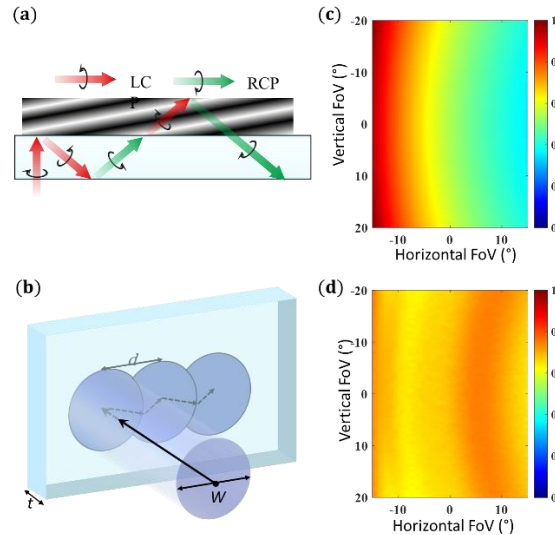


Figure 5. Polarization raytracing results of PVG as an in-coupler in waveguide displays. (a) Schematic of light propagation inside a waveguide around in-coupler region. (c) Angular response of PVG with birefringence of 0.4 at slanted angle of 23° and thickness of $0.7 \mu\text{m}$. (d) Improved in-coupling efficiency with optimized PVG by achieving the first order half-wave condition.

Due to the multiple interactions between incident light and conventional in-couplers [5-6], the theoretical in-coupling efficiency limit can be calculated based on the overlapping area (A_o) of the second interaction between the incident beam and the in-coupler, as depicted in Fig. 5(b). More specifically, the theoretical in-coupling efficiency limit (E) of a certain field can be expressed by the following equation:

$$E = 1 - \frac{A_o}{A_{in}} = 1 - \frac{2}{\pi} \cos^{-1} \left(\frac{d}{W} \right) + \frac{2d}{\pi W^2} \sqrt{W^2 - d^2} \quad (4)$$

where A_{in} is the area of in-coupler size or the exit pupil area of light engine. For instance, for the right-top corner FoV, it has a

maximum in-coupling efficiency limit of 100% since there is no second interaction between the incident light and the in-coupler. As indicated in Fig. 5(c), the minimum efficiency of the 50° FoV waveguide display is only around 36%, implying that only 36% of the in-coupling efficiency can be utilized to maintain good uniformity throughout the entire FoV.

To analyze how to improve the in-coupling efficiency and uniformity using PVG as an in-coupler, we conduct polarization ray-tracing simulations using OpticStudio (Ansys Zemax). The RCWA model of PVG is compiled into a dynamic-link library (DLL) file and linked to OpticStudio, operating in non-sequential mode. During the ray tracing process in Zemax OpticStudio, if a ray hits the grating with a DLL, RCWA is automatically called to solve the field response and provide return data. The mathematical construction process is detailed in our previous research [11]. To measure the in-coupling efficiency, an ideal grating is used as the out-coupler to couple all the light out of the waveguide. First, through optimizing the PVG thickness and slanted angle to satisfy the first order half-wave condition, the optimal efficiency and uniformity of the in-coupling process are achieved at 23° slanted angle and 0.7 μm thickness. Based on RCWA simulation, the average diffraction efficiency of the first interaction is around 80%. As shown in Fig. 4(d), after applying the optimized polarization conversion in PVG, the minimum in-coupling efficiency is improved from 36% to 61.3% (1.7x improvement) through polarization raytracing. Besides, the uniformity within the entire FoV is improved from 36% to 85.9% (2.39x improvement) if the following definition of uniformity U is adopted:

$$U = \frac{I_{\min}}{I_{\max}} * 100\% \quad (5)$$

where I_{\min} and I_{\max} represent the minimum and maximum brightness through the whole FoV, respectively. If the in-coupling efficiency of conventional couplers is also considered as 80%, then the in-coupling efficiency and uniformity will be improved by ~2x and ~2.3x, respectively.

4. Conclusion

We have discovered and demonstrated a novel polarization conversion phenomenon in polarization volume gratings. This breakthrough property effectively resolves the tradeoff between in-coupling efficiency and uniformity throughout the eyepiece and FoV. By studying the half-wave condition in PVG, we achieve a remarkable 2x improvement in in-coupling efficiency and 2.3x enhancement in uniformity across the FoV for a waveguide display with 50° FoV, compared to conventional couplers. Overall, this polarization conversion phenomenon serves as the first evidence to showcase the superiority of PVG in-coupler in waveguide-based AR displays compared to other couplers. This advancement is expected to accelerate the development of high-efficiency waveguide-based AR smart glasses and contribute to the commercialization of PVG technology.

5. Acknowledgments

The UCF group is indebted to Meta Reality Lab for financial support and Dr. Lu Lu for useful discussion.

6. References

1. Ding Y, Yang Q, Li Y, Yang Z, Wang Z, Liang H, Wu ST. Waveguide-based augmented reality displays: perspectives and challenges. *eLight*. 2023 Dec 7;3(1):24.
2. Kress BC, Chatterjee I. Waveguide combiners for mixed reality headsets: a nanophotonics design perspective. *Nanophotonics*. 2020 Dec 4;10(1):41-74.
3. Xiong J, Hsiang EL, He Z, Zhan T, Wu ST. Augmented reality and virtual reality displays: emerging technologies and future perspectives. *Light: Science & Applications*. 2021 Oct 25;10(1):1-30.
4. Ding Y, Gu Y, Yang Q, Yang Z, Huang Y, Weng Y, Zhang Y, Wu ST. Breaking the in-coupling efficiency limit in waveguide-based AR displays with polarization volume gratings. *Light: Science & Applications*. 2024 Aug 12;13(1):185.
5. Zhao Z, Lee YH, Feng X, Escuti MJ, Lu L, Silverstein B. Theoretical efficiency limit of diffractive input couplers in augmented reality waveguides. *Optics Express*. 2024 Mar 25;32(7):12340-57.
6. Goodsell J, Xiong P, Nikolov DK, Vamivakas AN, Rolland JP. Metagrating meets the geometry-based efficiency limit for AR waveguide in-couplers. *Optics Express*. 2023 Jan 30;31(3):4599-614.
7. Kobashi J, Yoshida H, Ozaki M. Planar optics with patterned chiral liquid crystals. *Nature Photonics*. 2016 Jun;10(6):389-92.
8. Weng Y, Xu D, Zhang Y, Li X, Wu ST. Polarization volume grating with high efficiency and large diffraction angle. *Optics Express*. 2016 Aug 8;24(16):17746-59.
9. Ding Y, Zhang Y, Ma Y, Huang Y, Wu ST. Polarization conversion effect in cholesteric liquid crystal-based polarization volume gratings. *Optics Express*. 2024 Nov 20;32(25):44425-36.
10. Xiong J, Wu ST. Rigorous coupled-wave analysis of liquid crystal polarization gratings. *Optics Express*. 2020 Nov 23;28(24):35960-71.
11. Ding Y, Li Y, Yang Q, Wu ST. Design optimization of polarization volume gratings for full-color waveguide-based augmented reality displays. *Journal of the Society for Information Display*. 2023 May;31(5):380-6.